Review Article **Open Access**

Stefan Droste*, Gabriel Ycas, Brian R. Washburn, Ian Coddington, and Nathan R. Newbury

Optical Frequency Comb Generation based on Erbium Fiber Lasers

DOI 10.1515/nanoph-2016-0019
Received October 16, 2015; accepted December 10, 2015

Abstract: Optical frequency combs have revolutionized optical frequency metrology and are being actively investigated in a number of applications outside of pure optical frequency metrology. For reasons of cost, robustness, performance, and flexibility, the erbium fiber laser frequency comb has emerged as the most commonly used frequency comb system and many different designs of erbium fiber frequency combs have been demonstrated. We review the different approaches taken in the design of erbium fiber frequency combs, including the major building blocks of the underlying mode-locked laser, amplifier, supercontinuum generation and actuators for stabilization of the frequency comb.

Keywords: optical frequency comb; fiber lasers; ultrafast optics; photonics

1 Introduction

A revolutionary breakthrough in the precise determination of optical frequencies was achieved in the late 1990s with the invention of the optical frequency comb technique [1–7]. An optical frequency comb allows a coherent connection between optical frequencies with 10^{15} cycles per second to radio frequencies, accessible and controllable with conventional electronics. The simple concept of optical frequency combs, their ease of operation, reliability, as well as versatility have turned them into a powerful tool that opens new frontiers in various fields of research [1, 2, 7–9] such as high-resolution spectroscopy, ultra-stable microwave generation, time and frequency transfer, astronomical spectrograph calibration, precision ranging, and, of course, optical atomic clocks.

The first demonstration of self-referenced frequency combs relied on passively mode-locked Ti:sapphire lasers [1–7]. Passively mode-locked lasers emit a periodic train of optical pulses in the time domain with a corresponding optical spectrum that consists of narrow spectral lines (or teeth), equidistantly spaced by the repetition rate, f_{rep}, of the laser. This entire comb of teeth is offset by the carrier-envelope-offset frequency, f_{ceo}. In this simple picture, the entire comb mode structure follows the comb equation $f_n = n \cdot f_{rep} + f_{ceo}$, where f_n is the frequency of the n^{th} numbered mode or comb tooth (typically n ~10^5–10^6). In order to use this simple equation, one must detect the carrier-envelope offset frequency, which, in turn, requires a low-noise, broad optical spectrum [5, 12]. The generation of an octave-spanning spectrum by the injection of Ti:sapphire laser pulses into a nonlinear "holey" fiber [13] was the breakthrough that allowed for the first demonstration of a self-referenced comb. The common description of an optical frequency comb is shown in Fig. 1.

With the advent of Ti:sapphire-based frequency combs, researchers were immediately interested in generating frequency combs from other lasers, in particular fiber-based passively mode-locked lasers. However, the direct output of femtosecond fiber lasers is inferior to Ti:sapphire mode-locked lasers as the pulses are of longer duration and suffer from higher relative intensity noise (RIN). Based on these considerations, it was not immediately obvious that a fiber laser-based frequency comb would be possible despite its obvious advantages in terms of cost, robustness, and flexibility. Specifically, given the decoherence observed during supercontinuum generation with a Ti:sapphire-based system [14–17], one might have expected the longer, noisier pulses of an erbium laser to generate a noisy supercontinuum so that the offset frequency would be undetectable. However, once appropriate nonlinear fibers were available [18–20], the development of fully self-referenced fiber laser frequency combs proceeded rapidly in several groups [21–26]. The linewidth of the detected offset frequency signal in the first erbium fiber combs was quite broad, for example, up to 600 kHz in Ref. 23, and partly because of these broad offset frequency

***Corresponding Author: Stefan Droste:** National Institute of Standards and Technology, 325 Broadway, Boulder, Colorado, 80305, USA; Email: stefan.droste@nist.gov; Tel.: +1 303-497-3475
Gabriel Ycas, Ian Coddington, Nathan R. Newbury: National Institute of Standards and Technology, 325 Broadway, Boulder, Colorado, 80305, USA
Brian R. Washburn: Department of Physics, Kansas State University, 116 Cardwell Hall, Manhattan, KS 66506, USA

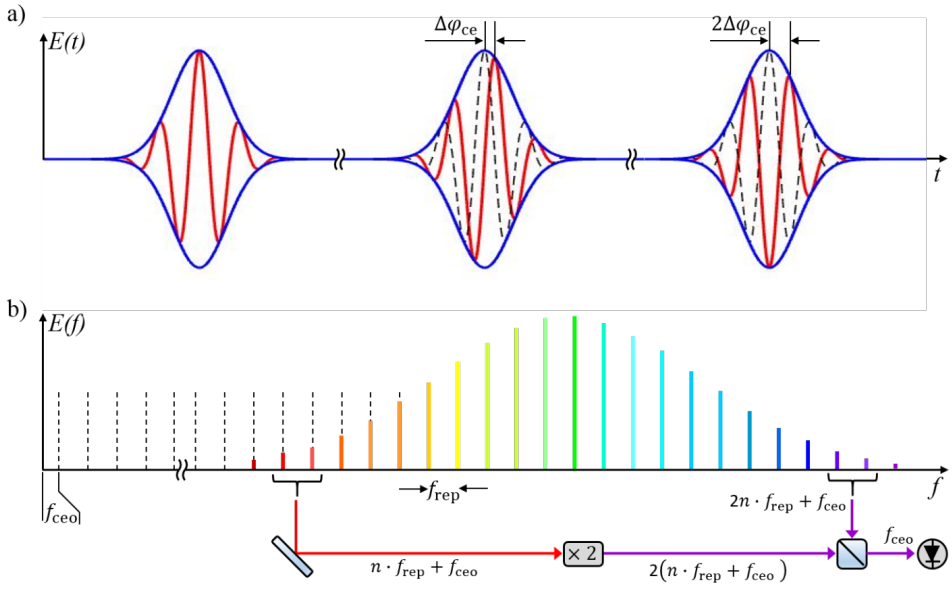

Figure 1: Optical pulse train and spectrum emitted by a mode-locked laser. a) The carrier wave (red) and the pulse envelope (blue) travel with different phase and group velocities, respectively, leading to a carrier-envelope phase shift, $\Delta\varphi_{ce}$, from pulse to pulse. b) The optical spectrum of a mode-locked laser is comprised of individual frequency teeth separated by the repetition rate, f_{rep}, of the laser. Extrapolating the spectrum to frequency zero reveals the offset, $f_{ceo} = f_{rep}\Delta\varphi_{ce}/(2\pi)$, which can also be regarded as the tooth at mode number $n = 0$. Also shown is the standard method of detecting f_{ceo} through an f-to-2f interferometer [5, 12].

linewidths, erbium fiber combs are sometimes considered to be noisier than their Ti:sapphire progenitors. However, one could argue that this is a misconception. First, the free-running linewidth of the detected offset frequency can be reduced by an order of magnitude through the use of a lower noise pump laser and by minimizing the cavity dispersion [27–33]. Second, this free-running phase noise is well-behaved in the sense that the basic comb structure is always preserved. Therefore, any residual performance deficit relative to Ti:sapphire-based combs can be removed through direct, high-bandwidth feedback of a correction signal to the fiber oscillator (or through signal processing). Indeed, as early as 2006, a collaboration between NIST, IMRA and OFS demonstrated time-bandwidth limited comb teeth linewidths of < 1 Hz from two very different comb designs [34]. Furthermore, early on both the phase noise and frequency stability of an erbium fiber frequency comb were shown to be comparable to that of a Ti:sapphire laser [35, 36]. With sufficient care in the design and stabilization of the erbium fiber frequency comb, it is rare that its frequency stability or phase noise is the limiting factor [36–38]. However, other properties of erbium combs, *for example*, the repetition rate, spectral flatness, robustness, size, spectral coverage, *etc.*, may still need advancement for current and future applications.

The development of erbium fiber frequency combs has been rapid and commercial systems are available (Menlo Systems [39], Toptica Photonics [40], IMRA America [41]). Moreover, the flexibility of the fiber-based platform and the ubiquity of low cost, high quality components in the erbium gain window has spurred research into different oscillator designs (see Sec. 3), multi-branch frequency combs [42–45], difference frequency generation to other wavelength bands [46–52], variable repetition-rate systems [53–56], synthesis of arbitrary optical frequencies [57–64], and robust fieldable systems [65–71]. In fact, one could argue that a significant majority of the demonstrations of comb applications have been done with erbium fiber lasers, driven largely by the rapidly maturing erbium comb technology.

This paper surveys different designs for erbium fiber-based frequency combs and is organized as follows. Section 2 summarizes the overall fiber frequency comb system. Section 3 discusses different passively mode-locked laser (or "oscillator") designs that form the core of the frequency comb. Section 4 outlines the supercontinuum generation needed for f-to-$2f$ detection of the offset frequency (and broad spectral coverage). Section 5 discusses the detection and stabilization of the comb lines. (We limit this review to frequency combs that are stabilized either by active feedback or by signal processing, rather than "free-running" frequency combs output by unstabilized, passively mode-locked lasers.) In this section, we also discuss different actuators used to control the comb output from

the oscillator. Section 6 briefly discusses the performance evaluation of frequency combs, emphasizing the importance of measuring the phase noise power spectral density rather than merely the linewidth of a signal.

2 Principles of optical frequency combs

Almost all self-referenced, stabilized frequency combs used thus far are generated by passively mode-locked lasers based on solid-state or fiber gain media such as erbium-doped fiber. There are several excellent review articles on passively mode-locked, femtosecond fiber lasers [72–75]. Erbium fiber-based mode-locked lasers produce a comb spectrum in the erbium gain window at around 1560 nm. Fiber frequency combs have also been developed with ytterbium [76] and thulium-doped fibers [77, 78] to reach other wavelength bands and to achieve high power levels. Although these thulium- and ytterbium-based systems are interesting in their own right, we focus here only on erbium fiber frequency combs, which have found the widest applications due to their combination of low cost, high performance, and compatibility with the myriad of components and tools available from the telecommunications industry.

The block diagram in Fig. 2 shows the subcomponents of a typical erbium fiber laser-based frequency comb system: a mode-locked laser oscillator, an amplifier, a spectral broadening section, a detection unit, and a feedback part or, alternatively, appropriate signal processing. The mode-locked laser emits a spectrally narrow and unstabilized frequency comb. The amplifier boosts the pulse energy and narrows the pulse duration so that the spectral broadening section provides up to a full optical octave as required for the detection of the offset frequency. At this point, the supercontinuum forms a free-running frequency comb; in other words, the frequency comb structure exists, but the exact optical frequency of each comb tooth is unknown and unstabilized. Equivalently, in the time domain, the pulse-to-pulse period and carrier-envelope phase evolution are not constrained. We define a stabilized comb as one where these values are known and, furthermore, any variations from noise sources—both external noise and amplified spontaneous emission (ASE)—have been canceled up to some effective control bandwidth. To stabilize the comb, we measure any two degrees of freedom. Three common examples are illustrated in Fig. 2: (1) the offset frequency, f_{ceo}, and the comb tooth spacing given by the repetition rate, f_{rep}, which stabilizes the comb to an rf reference [1, 2], (2) the offset frequency, f_{ceo}, and the frequency of a single optical comb tooth, f_{n0}, that stabilize the comb to an optical reference [6] or (3) the frequency of two widely spaced optical comb teeth, f_{n0} and f_{n1} [79–81], that effectively stabilize the comb to their frequency difference. Any noise is then canceled either through active feedback to the oscillator or through signal processing [32, 38, 82, 83]. The method of noise cancelation—(direct feedback, signal processing, or a combination)—is a matter of experimental choice.

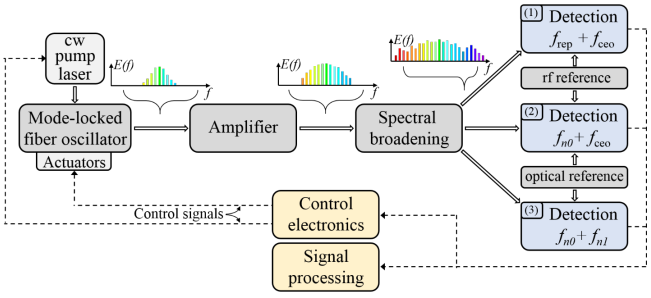

Figure 2: Block diagram of a typical fiber laser-based frequency comb system. The pulsed output of a fiber laser oscillator is amplified and spectrally broadened. These pulses are then launched into a highly nonlinear fiber in which nonlinear processes such as self-phase modulation, self-steepening, four-wave mixing, and Raman scattering spectrally broaden the pulses to a full octave. The detected signals are used in a control loop for the stabilization or they are combined with the experimental signals appropriately in signal processing to cancel out the comb noise. f_{n0}: frequency of a single optical comb tooth compared to an optical reference, f_{n1}: frequency of a single optical comb tooth compared to another optical reference.

3 Passively mode-locked erbium fiber lasers for frequency comb generation

As the core of the frequency comb, the ideal mode-locked laser would produce a high power, low RIN, and short, ~100 fs, pulses with very low free-running timing jitter and phase noise all in a completely self-starting, robust, easily reproducible package. Moreover, different applications will require different repetition rates ranging from 50 MHz to 1 GHz. Not surprisingly, no mode-locked fiber laser design possesses all of these features, and a number of different mode-locked erbium fiber laser designs have been

Table 1: Typical characteristics of demonstrated erbium fiber lasers used for stable frequency comb generation.

Oscillator design	Rep. rate [MHz]	Bandwidth [nm]	Ave. Power [mW]	Net cavity dispersion [ps^2]	Free-running f_{ceo} linewidth [kHz]	All-pm design?	Ref.
NPE ring	50–250	20–50	10–100	−0.04 to +0.04	10–1000	No	[11, 28, 29, 34, 38, 42–45, 55, 58, 81, 88, 89, 91–97]
Figure-8	20–50	10–20	1–10	−0.07 to −0.02	150–600	Yes	[23, 68, 98]
SAM linear	50–1000	~10	1–10	−0.012 to −0.02	40–1000	Yes	[25, 34, 67, 70, 99–104]
SAM ring	50–250	~10	1–10	−0.07 to −0.02	20–600	Yes	[69, 90, 105, 106]

NPE: nonlinear polarization evolution; SAM: saturable absorber mirror.

investigated. Fig. 3 and Table 1 provide a brief overview of some of the most common designs.

Regardless of the specific designs, all the passively mode-locked lasers share some commonalities. First, the erbium gain fiber within the mode-locked lasers is pumped with either 980 or 1480 nm laser diodes. Second, they all use a fast saturable absorption or saturable loss mechanism to enforce mode-locking. Third, they all have relatively narrow (10's of kHz) optical linewidths for the unstabilized frequency comb teeth near the center of the spectrum (1560 nm). These central comb teeth will have Schawlow–Townes linewidths equivalent to a cw laser at the same average power of the mode-locked laser [84] and equivalent sensitivity to environmentally induced cavity length variations [31]. Fourth, at high net cavity dispersion, their overall timing jitter (and f_{ceo} linewidth) will be dominated by the product of the dispersion and carrier-frequency noise through the Gordon–Haus effect [27, 30, 85–90]. At low net cavity dispersion, multiple other effects can dominate the timing jitter, including a direct ASE contribution [27, 30, 85–90]. A lower net cavity dispersion will also, generally, produce a broader output bandwidth, as can be seen from the general relationship between soliton spectral width and dispersion.

Beyond these commonalities, the oscillator designs and performances differ substantially as illustrated in Table 1 and discussed below. However, it is also important to note that virtually all erbium fiber comb designs also employ a very similar amplifier after the oscillator. This amplifier is what ultimately determines the pulse power and spectral width and greatly homogenizes the oscillator designs with respect to these two parameters.

3.1 Nonlinear polarization evolution mode-locked laser

To date, the most widely employed and extensively studied type of mode-locked erbium fiber laser is the nonlinear polarization evolution (NPE) mode-locked ring laser. A combination of the fiber birefringence and cross-phase modulation causes an intensity-dependent rotation of elliptically polarized light in standard single-mode fiber, *that is,* nonlinear polarization evolution [107–109]. When an appropriately aligned polarizing element is placed inside the cavity, an artificial saturable absorber can be created where light with higher intensity experiences lower losses through nonlinear polarization rotation. This effect favors pulsed over cw operation and stable mode-locking is achieved. Since the nonlinear polarization change occurs on femtosecond time scales, the artificial saturable absorber response is very fast. These lasers can be operated with a net negative or positive cavity dispersion giving rise to so-called "soliton" or "stretched pulse" operation [110, 111], respectively, with the stretched pulse regime tending to offer higher power and broader bandwidth.

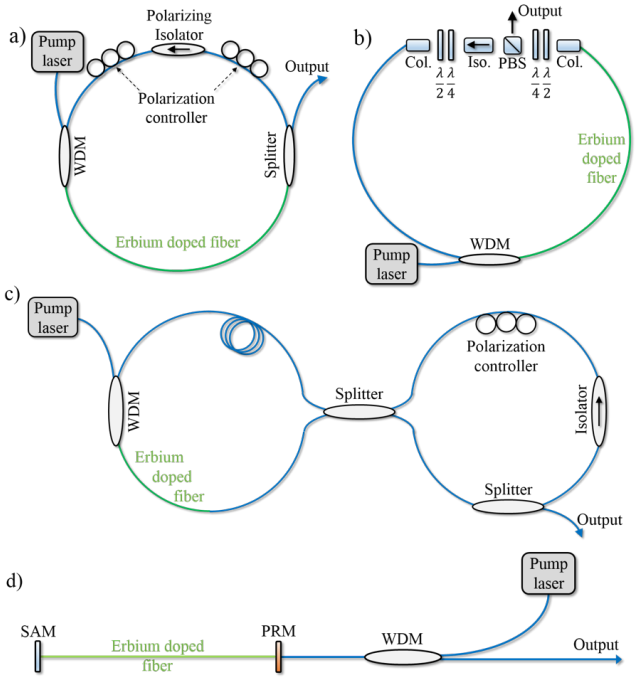

Figure 3: Some of the most widely used mode-locked erbium fiber oscillator designs. a) Simple ring laser based on nonlinear polarization evolution (NPE). The polarization controllers are adjusted in such a way that light with high intensity passes the polarizer while light with weaker intensity is blocked, therefore, favoring mode-locking operation. b) Modified NPE laser design that uses free-space optics for enhanced precision in polarization control. c) Figure-of-eight erbium fiber laser. The left side constitutes a nonlinear amplifying loop mirror (NALM). See text for details. d) Saturable absorber mirror (SAM) based mode-locked fiber laser. The SAM changes its reflectivity depending on the incident light intensity in such a way that the reflectivity increases with increasing intensity. Note that the oscillator designs of c) and d) support the use of polarization maintaining fiber components to provide a substantially higher degree of robustness and environmental immunity. WDM: wavelength division multiplexer, Col.: collimator, Iso.: isolator, PBS: polarizing beam splitter, $\lambda/2$: half wave plate, $\lambda/4$: quarter wave plate, PRM: partially reflecting mirror.

Fig. 3 a) shows a simple NPE-mode-locked erbium fiber laser based on the original design of Tamura *et al.* [112] while Fig. 3 b) shows an alternative design with a greater reliance on bulk optics. The all-fiber design is relatively quick to construct, given a fiber splicer, and comparably cheap. The bulk optic design allows one to use more precisely tunable or automated waveplates, and allows for easier tuning of the cavity length, but does add cost and requires careful alignment.

The downside of the NPE fiber laser is the susceptibility to environmental changes. Temperature fluctuations, humidity changes, or bending of the fibers introduce variations in the fiber birefringence, which alters the delicate balance between the NPE and the alignment of the various polarizing elements in the cavity thereby disrupting the artificial saturable absorber. Environmentally induced changes in fiber birefringence are often encountered in any fiber-optic system and can be eliminated by use of polarization maintaining (PM) fibers. However, the NPE requires polarization rotation and will not occur in PM fiber where the polarization is fixed along a predefined axis. Therefore, NPE fiber lasers are incompatible with a PM fiber design. While the environmentally induced instabilities can, nevertheless, be managed in a well-controlled laboratory, NPE lasers may never be appropriate for in-field or for unattended long-term operation. Additionally, different polarization settings can lead to different mode-locked states, which change the properties of the output pulses [89], making month-to-month operation highly variable. In spite of these drawbacks, NPE laser can operate at a large range of repetition rates, can be inexpensive, and can have low timing jitter making them an attractive laboratory option.

3.2 Figure-of-eight mode-locked laser

Another erbium fiber laser concept that is based on an all-fiber nonlinear loop mirror design was first demonstrated in the early 1990s [113–115]. Depicted in Fig. 3 (c), a passive resonator loop is coupled to a nonlinear amplifying loop mirror (NALM) that provides the gain and initiates the mode-locking. To understand the operation, consider a pulse circulating counterclockwise in the right passive loop (as allowed by the isolator). At the central 50/50 splitter, the pulse is split into two counter propagating pulses around the loop on the left side. In the absence of any nonlinear effects, when these counter propagating pulses interfere again at the 50/50 splitter, they "reflect" back (clockwise) out the initial input port, only to be rejected by the isolator. No light is transmitted through the other (lower) 50/50 port. However, the introduction of an amplification in the left loop forms a NALM and changes this behavior. In this case, the pulse traveling clockwise around the NALM is first amplified and then passes through passive fiber, while the light traveling counterclockwise first passes through passive fiber at low power and is then amplified. At sufficient pulse power, there is a differential nonlinear phase shift of π between these two pulses so that their interference at the 50/50 splitter does lead to transmission of the strong pulse from the (lower) port, opposite to the one the initial pulse entered. An isolator in the second loop ensures that lower-intensity reflected light is rejected, which provides the mode-locking mechanism.

A figure-of-eight erbium fiber laser can use all-PM fibers, making it alignment-insensitive and environmentally robust [68, 116]. Like NPE lasers, the nonlinear loop mirror is effectively a fast absorber and low-dispersion cavities can be constructed. A drawback of this laser design is that the mode-locking operation often is not self-starting. For this reason, electro-optic amplitude- or phase-modulators (EOM) are often used in order to initiate mode-locking. While these modulators make construction more challenging and expensive, once incorporated into the cavity an EOM can provide very fast feedback for low noise stabilization (discussed more in Sec. 5). The principle disadvantage of the figure-of-eight design is that it is complex. The large number of components in combination with a minimum loop mirror size necessary to get a π phase shift make it difficult to achieve a repetition rate above ~50 MHz—too low for many applications. More recently, an interesting variant of the figure-of-eight laser, called a "figure nine" laser, has been introduced by Menlo Systems [117]. This laser has been fully phase stabilized and very low residual phase noise could be demonstrated [118].

3.3 Saturable absorber-based mode-locked laser

3.3.1 Semiconductor saturable absorber mirror lasers

One of the simplest mode-locked erbium fiber laser concepts is a linear cavity realized by the use of a semiconductor saturable absorber mirror (SESAM) (see Fig. 3 d). A SESAM consists of a reflector whose front face is masked by a quantum well absorber layer. The quantum wells absorb light at the laser wavelength, but can be temporarily depleted, becoming transparent, in the presence of sufficiently high optical intensity [119, 120]. Shortly after a high intensity optical pulse hit the SESAM, the absorption recovers due to thermal relaxation and recombination processes. The recovery time is typically on the order of a few picoseconds and is an important design parameter of a SESAM.

Erbium fiber lasers that are mode-locked with a SESAM usually show excellent self-starting properties and a high degree of reproducibility. The laser cavity requires only the SESAM and a wavelength division multiplexer to introduce the pump light, making this one of the simplest cavity designs among all mode-locked erbium fiber lasers [67, 101]. When used in a linear configuration, the cavity length of a SESAM laser can be very short, and lasers with repetition rates above 1 GHz have been constructed [103, 121]. Additionally, this concept allows for an all-fiber and also all-PM design, which results in exceptionally robust and environmentally stable lasers [67].

The principle drawback of SESAM mode-locked lasers is that the SESAM is a slower saturable absorber than other designs and can require higher cavity dispersion in order to suppress parasitic ASE buildup in the wake of the pulse [122]. The timing jitter of the system can also be more affected by RIN [123] as the relatively slow saturable absorber introduces a temporal shift of the pulses inside the laser cavity; the magnitude of this shift is pulse energy-dependent so that pump laser intensity noise gets converted into timing jitter of the mode-locked pulses [87]. It should be noted that despite higher intrinsic noise with sufficiently fast feedback, the phase noise and timing jitter of a SESAM laser matches other stabilized combs [124].

3.3.2 Carbon nanotube and graphene saturable absorber lasers

Although saturable absorbers are mostly made from semiconductors, other materials can also be used. Two particularly interesting materials are carbon nanotubes (CNT) and graphene as their response time is sub-picosecond and, therefore, significantly faster than that of a SESAM. Additionally, both CNT and graphene are suitable for broadband operation covering a wide wavelength range from about 1 µm to 2 µm (CNT) and from the ultraviolet far into the infrared (graphene) [125]. However, both of these materials have high non-saturable losses as well as relatively low modulation depths, which present challenges. Additionally, at 1560 nm, the saturation fluence of graphene is not much below the material damage threshold, which can lead to problems if the laser Q-switches at start up. Nevertheless, mode-locked fiber lasers have been demonstrated with CNTs [90, 105, 126–129] as well as with graphene saturable absorbers [130–132]. A fully stabilized frequency comb system using CNTs deposited on a fiber tip has been reported [105], while only offset frequency stabilization has been demonstrated using a CNT embedded fiber taper [106]. Research efforts to exploit the potential of these materials are ongoing.

3.4 SESAM-NPE hybrid lasers

Inserting a SESAM into a NPE-based ring laser overcomes some of the limitations and drawbacks of a solely NPE mode-locked laser [133–135]. In this configuration, polarization states still must be aligned to benefit from the fast NPE process, however, optimization becomes easier with

the SESAM to initiate mode-locking. The SESAM also appears to suppress the long, low power wings in the time domain, providing a cleaner pulse structure [133]. While potentially more robust than lasers that only use NPE, this approach is still incompatible with PM fibers and will still have high environmental sensitivity.

4 Amplification, spectral broadening and offset frequency detection

As shown in Fig. 2, the laser oscillator is followed by an amplifier and a spectral broadening section for supercontinuum generation. The supercontinuum generation serves two purposes. First, it provides broad spectral coverage that might be needed for certain experiments or applications. Second, it enables the f-to-$2f$ detection of f_{ceo}, whereby a portion (~10 nm) of the long wavelength end of the supercontinuum is frequency-doubled and then heterodyned against the low wavelength end of the supercontinuum [5, 12] as sketched in Fig. 1 b). This approach requires a supercontinuum that covers a factor of two in frequency, commonly referred to as an octave-spanning spectrum. Typically, this scheme uses the two ends of the spectrum at around 1 and 2 μm (300–150 THz), although other methods have been demonstrated such as f-to-$2f$ from 785 to 1550 nm [24] and a $2f$-to-$3f$ interferometer [136, 137], which requires only 2/3 of an octave.

While researchers have explored a range of oscillator designs and stabilization approaches, post oscillator amplification is mostly done using very similar dispersion-managed erbium-doped fiber amplifiers. The amplifier is used to increase both the pulse energy and spectral width of the oscillator output and thus producing shorter, more intense pulses. There is significant flexibility in the design of an ultrafast erbium amplifier, which can employ temporal compression methods via self-similar amplification propagation [138], soliton self-compression [139–141], or a combination of both. These methods have the significant advantage of being constructed from fiber components fusion spliced together and are thus truly alignment-free. Essentially, the erbium amplifier compensates for a mediocre oscillator output and sub-100 fs pulses with ~1.5 nJ pulse energies can be achieved for all oscillator designs, despite the wide range of output powers and pulse durations evident in Table 1.

Typical amplifier designs as illustrated in Fig. 4 use high-gain, normal group-velocity dispersion (GVD) erbium-doped fibers. When correctly designed, the normal GVD of the erbium fiber, the fiber's gain and nonlinearity work together to allow the pulses undergoing amplification to spectrally broaden, while maintaining a linear chirp (i.e. a quadratic phase distortion). The pulses leaving the erbium-doped fiber amplifier will exhibit chirp, which must be removed for efficient supercontinuum generation. In a few cases, pulses leaving the gain fiber have negative chirp (the result of passing through material with net-anomalous GVD), which can be compensated for, by the use of a silicon prism compressor that exhibits normal GVD [21]. More commonly, the amplifier is designed with sufficient normal GVD so that the pulses have a positive chirp. This dispersion can be removed by adding anomalous GVD, either by the use of a grating compressor [138] or by simply passing the light through standard single-mode fiber [22, 25, 70, 106] or large mode-area optical fiber [139, 142]. For amplifiers employing solitonic compression methods, positively chirped pulses from the erbium-doped fiber with an energy greater than that of a fundamental soliton are injected into a length of anomalous GVD fiber. Here, the positive chirp is removed by the anomalous GVD increasing the pulse peak power to a point when nonlinear effects cause an increase in spectral bandwidth with a commensurate decrease in pulse duration.

To generate the supercontinuum required for f_{ceo} detection, the amplified pulses are injected into a highly nonlinear fiber (HNLF) [18, 143–145]. Obtaining a clean, low noise f_{ceo} signal requires a highly coherent supercontinuum. Decoherence of the supercontinuum appears as white phase noise that reduces the signal-to-noise ratio (SNR) of the f_{ceo} beat, and is caused by noise sources that are injected along with the input pulse, *that is*, shot noise and ASE, which mix with the laser field in the nonlinear fiber. As mentioned in the introduction, this decoherence was first identified with Ti:sapphire-based combs, where the input noise source was shot noise. Early studies of continuum coherence and amplitude noise found that for high-coherence spectra, it is important to launch sub-100 fs pulses into the HNLF with flat, slightly anomalous dispersion, and high effective nonlinearity (~10 W^{-1} km^{-1}) [15, 16, 19, 146]. There are now both non-PM and PM HNLF available that can produce an octave-spanning supercontinuum in a fiber length of ~10–30 cm. In addition to phase noise, supercontinuum generation can lead to strong amplitude noise. In that case, balanced photodetection of the f_{ceo} signal can increase the SNR by up to 20 dB [147].

In fiber combs, a collinear all-fiber-based f-to-$2f$ interferometer is usually used, which avoids losses from free-space coupling as well as non-common mode noise seen in

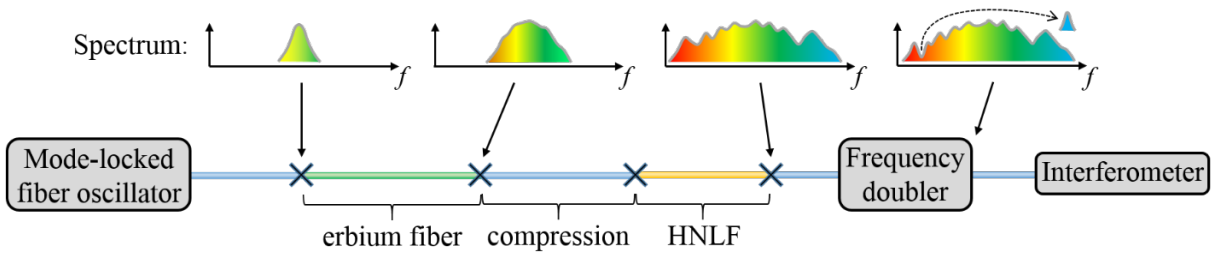

Figure 4: Common design of an amplifier including pulse compression for the supercontinuum generation in a highly nonlinear fiber. The frequency doubler is used to frequency double the long wavelength light. The doubled and the fundamental light is overlapped in the interferometer.

non-collinear interferometers [25]. Furthermore, compact and efficient commercial fiber-coupled periodically-poled lithium-niobate waveguide frequency doublers are available, which greatly simplifies and improves the f_{ceo} detection [102]. To stabilize the comb without "phase slips", the SNR of the detected f_{ceo} signal should exceed ~30 dB within a 300 kHz bandwidth and SNRs of 40 dB or more are now routinely achieved [25, 70, 102]. (Note that the required SNR is bandwidth-dependent).

5 Stabilization

5.1 Stabilization: The fixed point model

The frequency of each comb tooth is most often expressed with the simple relationship $f_n = n \cdot f_{rep} + f_{ceo}$. However, f_{ceo} and f_{rep} are not a natural basis set to describe the effects of noise or the influence of the actuators. Typically, changes in f_{ceo} and f_{rep} are strongly correlated. Specifically, nearly any noise source affects f_{rep}, even those commonly viewed as impacting f_{ceo}. An alternative description of the comb known as the elastic tape model, introduced by Telle and coworkers [82, 83], is more useful and captures the correlations across the comb spectrum [31, 32]. In this description, a given noise process or actuator will cause a comb tooth to expand or contract about a stationary point in frequency space known as the fixed point, f_{fix}. This fixed point may be within or even outside the optical comb spectrum (see Fig. 5).

Even within the elastic tape model, characterizing the comb noise is complicated since it is a highly nonlinear system. The main effects are summarized in Ref. 31. Any comb noise begins with an input noise seed that could be intracavity ASE, pump power fluctuations, pump spectrum fluctuations, temperature and humidity changes, mechanical vibrations, optical feedback, amplifier ASE, etc. The effect of these input noise seeds depends on the nonlinear coupled equations describing the comb output [27, 30, 86–88, 148]. For example, intracavity ASE will drive quantum-limited timing jitter and phase noise on the comb teeth. Variations in the power or spectrum of the laser diode that pumps the mode-locked fiber laser will lead to gain fluctuations that couple to the comb teeth position through self-steepening, resonant dispersion, self-phase modulation, third-order dispersion, carrier-frequency jitter coupled with cavity dispersion, and spectral-dependent loss. These different noise processes each tie back to their own fixed point. At the risk of oversimplifying the situation, one often categorizes the effects as follows: Temperature, humidity, and mechanical vibrations are all assumed to affect the cavity length leading to repetition rate changes with a fixed point of ~1 THz (given by the relative phase and group velocity of the fiber optics). Pump power and spectrum variations, quantum-limited timing jitter, and cavity loss variations are all assumed to affect the repetition rate with a fixed point near the carrier frequency of ~200 THz.

The combined contribution of all noise sources leads to linear variation of the frequency comb structure that must be measured and canceled. Since the comb structure is preserved, it is sufficient to detect the noise on two degrees-of-freedom of the comb as discussed in Sec. 5.2. As mentioned earlier, erbium fiber lasers often exhibit higher free-running noise than their solid-state counterparts, even at low net cavity dispersion. To suppress this noise, the detected signals are used to feed back correction signals to two actuators on the mode-locked laser, as discussed in more detail in Sec. 5.3. Alternatively, the detected signals can be included within the overall experiment's signal processing to remove the comb variations from the final output, as discussed in Sec. 5.4. Regardless, the goal is to effectively transform the noisy comb into a stable one that operates with sub-radian phase noise (with respect to the underlying oscillator), even below the quantum limit

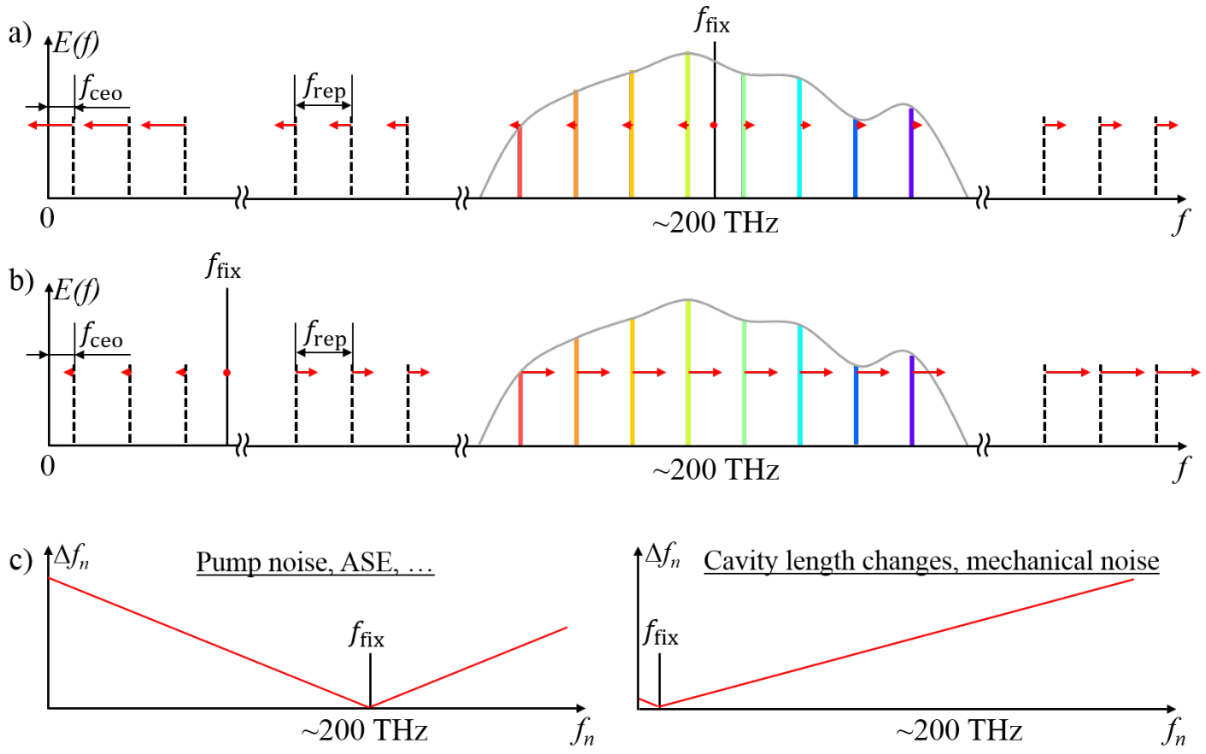

Figure 5: Fixed points, f_{fix}, of an erbium fiber frequency comb. Comb teeth under the optical spectrum (gray) are indicated by solid lines, while virtual teeth are indicated by dashed lines. a) For the case of pump power modulation, the fixed point is near the optical carrier frequency (~200 THz) with large tooth fluctuations (indicated by the length of the arrows) near 0 Hz. b) For the case of cavity length modulation via a piezo-electric transducer (PZT), the fixed point will be close to 0 Hz with large fluctuations at the optical carrier frequency. c) Depiction of the impact, Δf_n, of a given perturbation at different tooth frequencies, f_n, in the spectrum.

set by the intracavity ASE [31]. The ultimate performance is typically limited by the SNR of the detected signals and the actuator feedback bandwidth, or equivalently the latency in the signal processing.

5.2 Stabilization: Rf versus optical referencing

The measurement of two parameters is sufficient to capture the comb variations. Since these measurements will have limited SNRs, they should ideally span the frequency comb as widely as possible for the best sensitivity to the comb variations. Colloquially, this performance improvement with span is referred to as the "lever arm" associated with the measurement. (Likewise, if the comb is actively stabilized by feedback to two actuators, then the wider the span between the actuators' fixed points, the better.) Figure 2 shows three different options for measuring the comb noise: (1) pure rf stabilization, (2) rf and optical stabilization, and (3) a double-optical stabilization scheme.

For stabilization to an rf oscillator [e.g. case (1) of Fig. 2], one measures f_{ceo} and f_{rep}, which is not ideal as the measurement lever arm effectively spans a single comb tooth spacing. However, this approach can provide a simple and robust lock that provides a direct link between rf and optical frequencies. In practice, one usually stabilizes the comb to the p^{th} harmonic of f_{rep} in order to increase the lever arm. In the best case, the phase noise on the n^{th} optical comb tooth will be $20 \cdot \log(n/p)$ greater than the phase noise of the rf reference. While the average frequency of the comb teeth is indeed given by the standard formula $f_n = n \cdot f_{rep} + f_{ceo}$, the result of this fundamental noise multiplication is that the comb teeth themselves will have a broad linewidth as n/p ~10^4 to 10^6.

For stabilization to an optical oscillator [e.g. case (2) of Fig. 2], one measures f_{ceo} and the frequency of one optical comb tooth, f_{n0}, via its beat note with the optical oscillator [6]. In this case, the measurement lever arm spans the optical spectrum starting from the comb tooth at f_{n0} to the comb tooth at $n = 0$, namely f_{ceo}. (For a fully self-referenced lock, one stabilizes f_{ceo} to an rf frequency derived from the comb repetition rate.) The frequencies of the

comb teeth then are $f_n = f_{n0} + (n - n_0) f_{rep}$ where $f_{rep} = (f_{n0} - f_{ceo}) / n_0$. In that case, the phase noise of the optical reference is transferred to the optical comb teeth without the large multiplication factor present in the rf stabilization, leading to coherent comb teeth across the optical spectrum [34]. In optical frequency division applications, one then detects the repetition rate, which provides a microwave signal of a harmonic of the repetition rate since it has a phase noise that is $-20 \cdot \log(n/p)$ below the optical reference, which is a great example of the advantage of a large lever arm [149–151].

Finally, Fig. 2 shows a third option [case (3)] that circumvents the detection of f_{ceo} by pinning two optical comb teeth, f_{n0} and f_{n1}, to two optical standards possibly from two cw lasers locked to the same cavity. In that case, the comb tooth frequencies are $f_n = f_{n0} + n(f_{n1} - f_{n0}) / (n_1 - n_0)$. For cw lasers within the telecom band, $(n_1 - n_0) f_{rep}$ ~1 THz, giving a lever arm in between optical and rf stabilization with a resulting timing jitter that falls between the other two methods. More importantly, stabilization to an optical cavity provides narrow linewidths across the optical domain [31].

5.3 Stabilization by feedback

The two measurements of the comb variations are input to a proportional-integral-derivative controller and fed back to correct the initial comb output of the mode-locked laser via two or more actuators. Each actuator can be characterized by its bandwidth, *that is*, how fast changes can be applied, the modulation depth or dynamic range, and its fixed point (see Sec. 5.1). As a simple example, the modulation of the pump power (Fig. 5 a) typically has a fixed point near the center of the optical spectrum. It, therefore, has a large effect on the offset frequency near 0 Hz, far away from the optical domain. On the other hand, a modulation of the fiber cavity length using a piezo-electric transducer (PZT) will lead to a fixed point near 1 THz (Fig. 5 b), thus causing large fluctuations near the carrier frequency. Table 2 lists different actuators which are discussed in more detail below. In addition to the actuators of Table 2, other means of controlling the frequency comb degrees of freedom have been demonstrated, but are less commonly used [154, 155].

5.3.1 Actuators: Temperature control

The most basic environmental noise sources such as temperature, humidity, and mechanical vibrations cause variations in the intracavity optical path length and, therefore, in the repetition rate. Temperature control of the mode-locked laser can counteract these variations. It offers a high dynamic range, but is very slow. Therefore, temperature control is used in conjunction with other actuators such as a PZT or intracavity electro-optic modulator (EOM) that have much higher bandwidths, but limited dynamic range. If incorporated within the feedback system, temperature control can help ensure stabilization over long time scales and outside the well-controlled laboratory environment.

5.3.2 Actuators: Intracavity PZT

A PZT used as a fiber stretcher or mounted behind a cavity end mirror offers a moderately high bandwidth, inexpensive and simple actuator to control the cavity length. (To build a fiber stretcher, a small section of the intracavity fiber optic is epoxied to the side of the PZT.) The control bandwidth is 10's of kilohertz with minimal effort. At higher modulation frequencies, acoustic modes in the optical fiber or in the mounting structures can resonate, leading to large phase shifts that limit the achievable feedback bandwidth. However, with careful attention to the suppression of these resonances, bandwidths of 100 kHz or beyond are possible [67, 70, 156]. A single PZT requires large drive voltage to achieve moderate modulation depths, which is experimentally challenging. However, PZT "stacks" can provide large displacements while being driven at a more modest 0–100 V. It is also a common strategy to employ two PZT actuators: a slower PZT stack with a high modulation depth to handle long-term drifts and a faster PZT with lower modulation depth to counter acoustic transients.

5.3.3 Actuators: Gain/loss modulation—pump power and graphene loss modulator

One of the most widely used actuators is to vary the power of the laser diode that pumps the mode-locked laser. This approach has several advantages. First, erbium fiber oscillators are pumped with standard telecom laser diodes, which can be modulated at high frequencies with widely available drive electronics. Second, two important sources of noise—pump noise and intracavity ASE noise—have nearly the same fixed point as the pump modulation so that this actuator is well suited for suppressing this noise. As noted in Table 2, the fixed point is typically at ~200 THz, however, at low enough cavity dispersion, the fixed point can shift considerably [86]. The principal challenge with

Table 2: List of actuators used for the stabilization. Note that all values are approximate and for $f_{rep} = 100$ MHz; actual values can vary significantly depending on actuator and laser design.

Actuator	Bandwidth [kHz]	Modulation depth on f_{rep}	Fixed point [THz]	Representative references
Cavity length (Temperature)	< 0.001	1 kHz/K	~1	[152]
Pump power modulation	10–1000	20 Hz/mW	~200	[28, 88, 97]
Cavity length (PZT)	1–100	0.1–10 kHz	0–1	[70, 88]
EOM	500–4000	100 Hz	~1–100	[44, 68, 96, 97, 124, 153]
AOM	100–1000	0 Hz (5–10) MHz only on f_{ceo})	∞	[91]
Graphene	1000	~10 Hz	~200	[124]

PZT: piezo-electric transducer; EOM: electro-optic modulator; AOM: acousto-optic modulator.

pump modulation is that the erbium stimulated emission time constant is slow, leading to a roll-off in the pump response around 10 kHz. However, this roll-off appears as a simple RC time constant so that with appropriate phase lead compensation techniques [28, 29], feedback bandwidths as high as 900 kHz have been demonstrated with custom electronic circuits [97].

One can also directly modulate the intracavity loss (rather than modulate the intracavity gain through the pump power). Loss modulation has the same fixed points, but a larger bandwidth and has been demonstrated with graphene modulators [157]. Here, the absorptivity of a graphene sheet is modulated by a few percent with an applied electric field. A graphene modulator was first used to stabilize the offset frequency of a thulium-fiber comb [77] and, more recently, an erbium-fiber-based frequency comb with a control bandwidth of over 1 MHz [124].

5.3.4 Actuators: Intracavity EOM

Widely employed in fiber communications, lithium-niobate, electro-optic phase modulators (EOM) offer an obvious and extremely high bandwidth means of modulating an erbium comb [44, 68, 81, 96, 97, 124, 153]. The refractive index of the EOM crystal changes proportionally to an applied voltage by a few parts in 10^6, which represents a change in cavity length and, therefore, in the repetition rate. EOMs are available as bulk-optic crystals or fully fiber-coupled waveguide devices. The fiber-coupled waveguide EOMs require no alignment, have very high bandwidths (> 10's of MHz), and low drive voltages, but often have 2 dB or more of insertion loss. Waveguide EOMs have achieved control bandwidths of over 2 MHz [81], providing modulation on timescales shorter than even the cavity photon lifetime [77]. Bulk-optic EOMs require a free-space section in the laser cavity as well as a high drive voltage, and can have limited bandwidth due to acoustic resonances or limitations in the high voltage driver, but they have less insertion loss and introduce less third-order dispersion by virtue of being a shorter crystal.

Unfortunately, the challenges associated with EOMs also merit mention. In addition to their expense, insertion loss, and added third-order dispersion, the largest issue is the fixed point frequency. For a waveguide EOM, the fixed point can be as high as ~50–100 THz [81], which is inconveniently located between the fixed points of other actuators and the main noise sources. Therefore, feedback through this EOM can lead to cross-talk. Furthermore, this fixed point is not necessarily independent of the modulation frequency. Thermal effects can lead to a low fixed point near DC, while electro-optic effects lead to a different fixed point at higher frequencies [153]. EOMs have been most successfully employed for optical frequency division applications where high bandwidth is needed and only f_{rep} has to be stabilized. Therefore, one can feed back on the difference between f_n and f_{ceo} so that the fixed point becomes irrelevant [81, 150, 151, 153]. However, when coupled with a high-bandwidth pump current modulation, EOMs have also effectively reduced phase noise degradation in dual-comb spectroscopy experiments [158].

5.3.5 Actuators: External acousto-optic modulators

External cavity AOMs (i.e. an AOM located at the output of the mode-locked laser) are distinct in that they have no impact on f_{rep} and provide a pure translation of the comb [91, 159]. A significant advantage of an AOM is the speed. An AOM constructed so that the beam passes close

to the transducer can achieve 1 MHz of feedback bandwidth and nearly any AOM can achieve a 100 kHz bandwidth. Also, as an external cavity device, it can be used with no impact on the mode-locking although it can spectrally filter the output depending on its optical bandwidth. The down side of an AOM is that its fixed point is effectively at infinity and does not correspond to any noise source. An AOM must be used in conjunction with another modulator to truly cancel most noise sources.

5.3.6 Actuators: Difference frequency generation

Though not technically an actuator, difference frequency generation (DFG) in a nonlinear crystal can be used to simply force f_{ceo} to zero [160–162]. In the DFG, f_{ceo} drops out of the final comb due to the subtraction. In the final f_{ceo}-free DFG comb, there is then only one degree of freedom and the fixed point of all noise sources and actuators is forced to 0 Hz. Therefore, a full stabilization of the comb only requires a single actuator acting on f_{rep}. Much like the AOM, this is an extracavity approach that is compatible with any mode-locked laser. Moreover, DFG between different parts of the comb's spectrum generates light in other interesting spectral regions such as the mid-IR and far-IR [47, 48, 50–52, 163], or just regenerates light in the near-IR.

5.4 Stabilization by processing

Once the comb fluctuations are quantified, it is technically not necessary to feed back a correction signal in order to stabilize the comb since the measured fluctuations can be appropriately scaled and simply subtracted from the final measurement data. This is known as the "transfer oscillator concept" originally demonstrated by Telle *et al.* and allows for strong suppression of the frequency comb noise [36, 82]. This approach has an advantage over active feedback in that the noise cancelation is no longer limited by the bandwidth of the actuators and, in principle, is only limited by the latency in the signal processing.

In practice, some sort of slow feedback is also needed to manage long timescales, so that the various detected rf signals remain within their effective processing bandwidth. Therefore, some sort of intermediate approach is often taken where a slow feedback maintains the approximate comb position and signal processing is used to remove the higher frequency fluctuations. A nice example of this approach occurs in microwave generation where f_{rep} is isolated and stabilized by detecting and signal processing f_{ceo} and f_n [150, 164]. Variations have been applied to both dual-comb spectroscopy [80, 165, 166] and in low noise optical frequency transfer [38].

6 Frequency comb performance evaluation

The performance of a comb is dictated by the absolute phase noise of the underlying optical or rf reference plus any residual phase noise between the comb and this reference. Often, only the residual noise is given in the comb literature as the noise of the absolute reference is unrelated to the comb itself. There are a number of different measures: the residual phase noise on f_{ceo}, the residual phase noise on an optical comb tooth (f_n), the residual phase noise on f_{rep} or equivalently the pulse-to-pulse timing jitter, the residual Allan deviation of a comb tooth or the repetition rate (i.e. the stability), the optical comb tooth linewidth or the fractional power in the carrier for a given tooth.

The phase noise represents the most fundamental measurement. It is quantified by the phase noise power spectral density (PSD), in units of rad^2/Hz or dBc/Hz, versus Fourier frequency. As a comb has only two free parameters, the phase noise PSD of any two comb components are sufficient to at least estimate the noise of any other comb component (along with an assumption about correlations). For a comb stabilized to an optical reference, the residual phase noise PSD of f_{ceo} or f_n is measured by demodulating the respective rf heterodyne signal. For a comb stabilized to an rf reference, the residual phase noise PSD of f_{ceo} and f_{rep} are similarly recorded. The phase noise PSD can be very helpful in identifying different noise sources. Moreover, the integrated phase noise is a useful single number (linewidth-like) metric provided that the upper and lower Fourier frequencies for the integration are given. (Note that the frequency noise PSD is obtained from the phase noise PSD by simply scaling by f^2, where f is the Fourier frequency.) If the phase noise is measured for the same rf signal used to control the comb, then the phase noise PSD is considered "in loop" and represents a best case value. More realistic "out-of-loop" measurements require some distinct measurement of the comb noise.

In principle, the Allan deviation can be calculated directly from an integral over the phase noise [167, 168] although it is typically calculated instead from frequency counter data for the evaluation of the long-term stability since phase noise PSDs are rarely acquired at sufficiently low Fourier frequencies. "In loop" measurements of the Allan deviation are of limited utility since "out-of-loop" fiber

and air paths that vary slowly with room temperature variations often dominate and must be taken into account.

The comb tooth linewidth is also sometimes quoted, but the linewidth is of limited use for optically referenced combs. Although it is a readily measured and seemingly intuitive number, there are three problems associated to the linewidth. First, the linewidth can depend heavily on the observation time. Second, as a single number, it conveys basically no information about the magnitude or frequency of the contributing noise. Third, it is a highly nonlinear measure of the phase noise. Specifically, for an optically referenced comb with integrated optical phase noise below ~1 radian (or 0.69 radians strictly speaking), the power spectrum of a comb tooth collapses to a single coherent peak atop a broader noise pedestal [169]. The full-width at half maximum linewidth is fundamentally time-bandwidth limited. The comb system is, after all, a phase-locked system. Any linewidth measurements under these conditions will be limited either by the measurement instrument or by optical path variations after the comb itself and of little meaning.

The "power in the carrier" is a similar nonlinear measurement of the phase noise, but of more use than the linewidth since it quantifies the percent of power in the coherent carrier versus the pedestal. When there is a coherent carrier, the fractional power in this carrier is given by $\exp\left(-\sigma_n^2\right)$ where σ_n^2 is the integrated phase noise for the comb tooth under consideration [34, 169]. In other words, it is equivalent to quoting the integrated phase noise.

Finally, the pulse-to-pulse timing jitter is a useful time domain description. Of course, it is also the noise on the comb tooth spacing or repetition rate and is, therefore, simply a scaled version of the phase noise PSD of f_{rep} [168]. Residual timing jitter is often in the few femtosecond to 100 attosecond range so that a very sensitive measurement is needed such as the balanced cross-correlator technique [170] or comparison of a high harmonic of f_{rep} to a very quiet rf oscillator. However, to avoid these challenges as well as the excess noise present in photodetection, one can estimate the timing jitter, δt_{pulse}, from optical measurements. Specifically, the residual timing jitter can be derived from the residual phase noise measurements of f_{ceo} and f_n by the equation $2\pi\delta t_{pulse} = \left(\sigma_n^2 + \sigma_{ceo}^2\right)^{1/2} / \left(f_n - f_{ceo}\right)$ where σ_n and σ_{ceo} is the integrated residual phase noise on f_n and f_{ceo} in radians, respectively, and assuming uncorrelated noise.

7 Summary

Erbium fiber laser frequency combs have matured rapidly through extensive research and now offer great flexibility in design, construction, and output properties. The higher noise level associated with erbium combs compared to bulk laser combs can be compensated by utilizing high bandwidth actuators for efficient noise compensation, by appropriate signal processing or a combination of these two. Furthermore, advances in erbium fiber combs continue with research in areas such as the use of CNT for fast saturable absorbers, graphene for high-bandwidth loss modulation, and robust optical designs. Given the long list of applications for frequency combs, we expect to witness a continued development of erbium fiber combs and a continued expansion of their use in both the metrology laboratory and fielded sensor systems.

Acknowledgement: The authors would like to thank Frank Quinlan, Holly Leopardi, and Curtis Menyuk for helpful discussions. The use of trade names in this article is necessary for completeness and does not constitute an endorsement by the National Institute of Standards and Technology.

References

[1] J. L. Hall, "Nobel Lecture: Defining and measuring optical frequencies," Rev. Mod. Phys. **78**(4), 1279–1295 (2006).

[2] T. W. Hänsch, "Nobel Lecture: Passion for precision," Rev. Mod. Phys. **78**(4), 1297–1309 (2006) [doi:10.1103/RevModPhys.78.1297].

[3] R. Holzwarth et al., "Optical Frequency Synthesizer for Precision Spectroscopy," Phys. Rev. Lett. **85**(11), 2264–2267 (2000) [doi:10.1103/PhysRevLett.85.2264].

[4] S. A. Diddams et al., "Direct Link between Microwave and Optical Frequencies with a 300 THz Femtosecond Laser Comb," Phys. Rev. Lett. **84**(22), 5102–5105 (2000) [doi:10.1103/PhysRevLett.84.5102].

[5] D. J. Jones et al., "Carrier-Envelope Phase Control of Femtosecond Mode-Locked Lasers and Direct Optical Frequency Synthesis," Science **288**(5466), 635–639 (2000) [doi:10.1126/science.288.5466.635].

[6] S. A. Diddams et al., "An Optical Clock Based on a Single Trapped 199Hg+ Ion," Science **293**(5531), 825–828 (2001).

[7] S. T. Cundiff and J. Ye, "Colloquium: Femtosecond optical frequency combs," Rev Mod Phys **75**(1), 325–342 (2003) [doi:10.1103/RevModPhys.75.325].

[8] N. R. Newbury, "Searching for applications with a fine-tooth comb," Nat. Photon **5**(4), 186–188 (2011).

[9] S. A. Diddams, "The evolving optical frequency comb [Invited]," J. Opt. Soc. Am. B **27**(11), B51–B62 (2010) [doi:10.1364/JOSAB.27.000B51].

[10] T. Udem et al., "Accurate measurement of large optical frequency differences with a mode-locked laser," Opt. Lett. **24**(13), 881–883 (1999) [doi:10.1364/OL.24.000881].
[11] F. R. Giorgetta et al., "Optical two-way time and frequency transfer over free space," Nat. Photonics **7**(6), 434–438 (2013) [doi:10.1038/nphoton.2013.69].
[12] H. R. Telle et al., "Carrier-envelope offset phase control: A novel concept for absolute optical frequency measurement and ultrashort pulse generation," Appl Phys B **69**(4), 327–332 (1999).
[13] J. K. Ranka, R. S. Windeler, and A. J. Stentz, "Visible continuum generation in air-silica microstructure optical fibers with anomalous dispersion at 800 nm," Opt. Lett. **25**(1), 25 (2000) [doi:10.1364/OL.25.000025].
[14] M. Nakazawa et al., "Coherence Degradation in the Process of Supercontinuum Generation in an Optical Fiber," Opt Fiber Techn **4**, 215–223 (1998).
[15] K. L. Corwin et al., "Fundamental noise limitations to supercontinuum generation in microstructure fiber," Phys Rev Lett **90**(11), 113904 (2003).
[16] N. R. Newbury et al., "Noise amplification during supercontinuum generation in microstructure fiber," Opt Lett **28**(11), 944–946 (2002).
[17] J. M. Dudley, G. Genty, and S. Coen, "Supercontinuum generation in photonic crystal fiber," Rev. Mod. Phys. **78**(4), 1135–1184 (2006) [doi:10.1103/RevModPhys.78.1135].
[18] J. W. Nicholson et al., "All-fiber, octave-spanning supercontinuum," Opt. Lett. **28**(8), 643 (2003) [doi:10.1364/OL.28.000643].
[19] J. W. Nicholson and M. F. Yan, "Cross-coherence measurements of supercontinua generated in highly-nonlinear, dispersion shifted fiber at 1550 nm," Opt. Express **12**(4), 679 (2004) [doi:10.1364/OPEX.12.000679].
[20] N. Nishizawa and T. Goto, "Widely Broadened Super Continuum Generation Using Highly Nonlinear Dispersion Shifted Fibers and Femtosecond Fiber Laser," Jpn. J. Appl. Phys. **40**(Part 2, No. 4B), L365–L367 (2001) [doi:10.1143/JJAP.40.L365].
[21] F. Tauser, A. Leitenstorfer, and W. Zinth, "Amplified femtosecond pulses from an Er:fiber system: Nonlinear pulse shortening and self-referencing detection of the carrier-envelope phase evolution," Opt. Express **11**(6), 594–600 (2003) [doi:10.1364/OE.11.000594].
[22] B. R. Washburn et al., "An all-fiber, phase-locked supercontinuum source for frequency metrology," presented at Frontiers in Optics, 2003, PostDeadline Paper 7, OSA [doi:10.1364/FIO.2003.PDP7].
[23] B. R. Washburn et al., "Phase-locked, erbium-fiber-laser-based frequency comb in the near infrared," Opt Lett **29**(3), 250–252 (2004).
[24] H. Hundertmark et al., "Phase-locked carrier-envelope-offset frequency at 1560 nm," Opt. Express **12**(5), 770 (2004) [doi:10.1364/OPEX.12.000770].
[25] T. R. Schibli et al., "Frequency metrology with a turnkey all-fiber system," Opt Lett **29**(21), 2467–2469 (2004) [doi:10.1364/OL.29.002467].
[26] P. Kubina et al., "Long term comparison of two fiber based frequency comb systems," Opt. Express **13**(3), 904–909 (2005) [doi:10.1364/OPEX.13.000904].
[27] H. A. Haus and A. Mecozzi, "Noise of mode-locked lasers," IEEE J. Quantum Electron. **29**(3), 983–996 (1993) [doi:10.1109/3.206583].
[28] J. J. McFerran et al., "Elimination of pump-induced frequency jitter on fiber-laser frequency combs," Opt Lett **31**(13), 1997–1999 (2006).
[29] J. J. McFerran et al., "Suppression of pump-induced frequency noise in fiber-laser frequency combs leading to sub-radian f (ceo) phase excursions," Appl Phys B **86**(2), 219–227 (2007).
[30] R. Paschotta et al., "Optical phase noise and carrier-envelope offset noise of mode-locked lasers," Appl. Phys. B **82**(2), 265–273 (2005) [doi:10.1007/s00340-005-2041-9].
[31] N. R. Newbury and W. C. Swann, "Low-noise fiber-laser frequency combs (Invited)," J Opt Soc Am B **24**(8), 1756–1770 (2007).
[32] E. Benkler et al., "Circumvention of noise contributions in fiber laser based frequency combs," Opt. Express **13**(15), 5662–5668 (2005).
[33] T. K. Kim et al., "Sub-100-as timing jitter optical pulse trains from mode-locked Er-fiber lasers," Opt. Lett. **36**(22), 4443–4445 (2011) [doi:10.1364/OL.36.004443].
[34] W. C. Swann et al., "Fiber-laser frequency combs with subhertz relative linewidths," Opt Lett **31**(20), 3046–3048 (2006).
[35] I. Coddington et al., "Coherent optical link over hundreds of metres and hundreds of terahertz with subfemtosecond timing jitter," Nat. Photonics **1**(5), 283–287 (2007) [doi:10.1038/nphoton.2007.71].
[36] L. A. M. Johnson, P. Gill, and H. S. Margolis, "Evaluating the performance of the NPL femtosecond frequency combs: agreement at the 10^{-21} level," Metrologia **52**(1), 62–71 (2015) [doi:10.1088/0026-1394/52/1/62].
[37] F. Quinlan et al., "Optical amplification and pulse interleaving for low-noise photonic microwave generation," Opt. Lett. **39**(6), 1581 (2014) [doi:10.1364/OL.39.001581].
[38] D. Nicolodi et al., "Spectral purity transfer between optical wavelengths at the 10-18 level," Nat. Photonics **8**(3), 219–223 (2014) [doi:10.1038/nphoton.2013.361].
[39] http://www.menlosystems.com/
[40] http://www.toptica.com/
[41] http://www.imra.com/
[42] F. Adler et al., "Phase-locked two-branch erbium-doped fiber laser system for long-term precision measurements of optical frequencies," Opt Express **12**(24), 5872–5880 (2004).
[43] G. Ycas, S. Osterman, and S. A. Diddams, "Generation of a 660–2100 nm laser frequency comb based on an erbium fiber laser," Opt. Lett. **37**(12), 2199 (2012) [doi:10.1364/OL.37.002199].
[44] Y. Nakajima et al., "A multi-branch, fiber-based frequency comb with millihertz-level relative linewidths using an intracavity electro-optic modulator," Opt. Express **18**(2), 1667–1676 (2010) [doi:10.1364/OE.18.001667].
[45] F. Adler et al., "Attosecond relative timing jitter and 13 fs tunable pulses from a two-branch Er: fiber laser," Opt Lett **32**(24), 3504–3506 (2007).
[46] P. Maddaloni et al., "Mid-infrared fibre-based optical comb," New J. Phys. **8**(11), 262 (2006) [doi:10.1088/1367-2630/8/11/262].
[47] C. Erny et al., "Mid-infrared difference-frequency generation of ultrashort pulses tunable between 3.2 and 4.8 μm from a compact fiber source," Opt. Lett. **32**(9), 1138–1140 (2007)

[doi:10.1364/OL.32.001138].
[48] P. Maddaloni, P. Cancio, and P. De Natale, "Optical comb generators for laser frequency measurement," Meas Sci Technol **20**(5), 052001 (2009).
[49] E. Baumann et al., "Spectroscopy of the methane ν_3 band with an accurate midinfrared coherent dual-comb spectrometer," Phys. Rev. A **84**(6), 062513 (2011) [doi:10.1103/PhysRevA.84.062513].
[50] F. Keilmann and S. Amarie, "Mid-infrared Frequency Comb Spanning an Octave Based on an Er Fiber Laser and Difference-Frequency Generation," J. Infrared Millim. Terahertz Waves **33**(5), 479–484 (2012) [doi:10.1007/s10762-012-9894-x].
[51] F. Zhu et al., "High-power mid-infrared frequency comb source based on a femtosecond Er:fiber oscillator," Opt. Lett. **38**(13), 2360–2362 (2013) [doi:10.1364/OL.38.002360].
[52] F. C. Cruz et al., "Mid-infrared optical frequency combs based on difference frequency generation for molecular spectroscopy," Opt. Express **23**(20), 26814 (2015) [doi:10.1364/OE.23.026814].
[53] K. Minoshima and H. Matsumoto, "High-accuracy measurement of 240-m distance in an optical tunnel by use of a compact femtosecond laser," Appl Opt **39**(30), 5512–5517 (2000).
[54] H. Hundertmark et al., "Stable sub-85 fs passively mode-locked Erbiumfiber oscillator with tunable repetition rate," Opt. Express **12**(14), 3178–3183 (2004) [doi:10.1364/OPEX.12.003178].
[55] B. Washburn et al., "Fiber-laser-based frequency comb with a tunable repetition rate," Opt Express **12**(20), 4999–5004 (2004).
[56] Y. Liu et al., "Low-timing-jitter, stretched-pulse passively mode-locked fiber laser with tunable repetition rate and high operation stability," J. Opt. **12**(9), 095204 (2010) [doi:10.1088/2040-8978/12/9/095204].
[57] T. R. Schibli et al., "Phase-locked widely tunable optical single-frequency generator based on a femtosecond comb," Opt Lett **30**(17), 2323–2325 (2005).
[58] Y.-J. Kim et al., "All-fiber-based optical frequency generation from an Er-doped fiber femtosecond laser," Opt Express **17**(13), 10939–10945 (2009).
[59] Y.-J. Kim et al., "Generation of optical frequencies out of the frequency comb of a femtosecond laser for DWDM telecommunication," Laser Phys. Lett. **7**(7), 522 (2010) [doi:10.1002/lapl.201010012].
[60] F. Rohde, E. Benkler, and H. R. Telle, "High contrast, low noise selection and amplification of an individual optical frequency comb line," Opt. Lett. **38**(2), 103 (2013) [doi:10.1364/OL.38.000103].
[61] E. Benkler, F. Rohde, and H. R. Telle, "Endless frequency shifting of optical frequency comb lines," Opt. Express **21**(5), 5793 (2013) [doi:10.1364/OE.21.005793].
[62] I. Coddington et al., "Characterizing Fast Arbitrary CW Waveforms with 1500 THz/s Instantaneous Chirps," IEEE J Sel Top. Quantum Electron **18**(1), 228–238 (2012).
[63] J. Jost, J. Hall, and J. Ye, "Continuously tunable, precise, single frequency optical signal generator," Opt. Express **10**(12), 515–520 (2002) [doi:10.1364/OE.10.000515].
[64] V. Ahtee, M. Merimaa, and K. Nyholm, "Single-frequency synthesis at telecommunication wavelengths," Opt Express **17**(6), 4890–4896 (2009).
[65] Y.-J. Kim et al., "Development of Fiber Femtosecond Lasers for Advanced Metrological Space Missions," presented at The 10th Conference on Lasers and Electro-Optics Pacific Rim, 2013, Kyoto, Japan, Optical Society of America.
[66] T. Wilken et al., "A frequency comb and precision spectroscopy experiment in space," in CLEO:2013, p. AF2H.5, Optical Society of America, San Jose (2013) [doi:10.1364/CLEO_AT.2013.AF2H.5].
[67] L. C. Sinclair et al., "Operation of an optically coherent frequency comb outside the metrology lab," Opt. Express **22**(6), 6996–7006 (2014) [doi:10.1364/OE.22.006996].
[68] E. Baumann et al., "High-performance, vibration-immune fiber-laser frequency comb," Opt Lett **34**(5), 638–640 (2009).
[69] J. Lee et al., "Testing of a femtosecond pulse laser in outer space," Sci. Rep. **4** (2014) [doi:10.1038/srep05134].
[70] L. C. Sinclair et al., "Invited Article: A compact optically coherent fiber frequency comb," Rev. Sci. Instrum. **86**(8), 081301 (2015) [doi:10.1063/1.4928163].
[71] M. Lezius et al., "Frequency comb metrology in space," presented at 8th Symposium on Frequency Standards and Metrology, 2015, Potsdam, Germany.
[72] L. Nelson et al., "Ultrashort-pulse fiber ring lasers," Appl Phys B **65**(2), 277–294 (1997) [doi:10.1007/s003400050273].
[73] M. E. Fermann and I. Hartl, "Ultrafast Fiber Laser Technology," IEEE J Sel Top. Quantum Electron **15**(1), 191–206 (2009) [doi:10.1109/JSTQE.2008.2010246].
[74] M. E. Fermann and I. Hartl, "Fiber laser based hyperspectral sources," Laser Phys. Lett. **6**(1), 11 (2009) [doi:10.1002/lapl.200810090].
[75] M. E. Fermann and I. Hartl, "Ultrafast fibre lasers," Nat. Photonics **7**(11), 868–874 (2013) [doi:10.1038/nphoton.2013.280].
[76] A. Ruehl, "Advances in Yb:Fiber Frequency Comb Technology," Opt. Photonics News **23**(5), 30 (2012) [doi:10.1364/OPN.23.5.000030].
[77] C.-C. Lee et al., "Frequency comb stabilization with bandwidth beyond the limit of gain lifetime by an intracavity graphene electro-optic modulator," Opt. Lett. **37**(15), 3084 (2012) [doi:10.1364/OL.37.003084].
[78] J. Jiang et al., "Fully stabilized, self-referenced thulium fiber frequency comb," in Lasers and Electro-Optics Europe (CLEO EUROPE/EQEC), 2011 Conference on and 12th European Quantum Electronics Conference, pp. 1–1 (2011) [doi:10.1109/CLEOE.2011.5943710].
[79] I. Coddington, W. C. Swann, and N. R. Newbury, "Coherent multiheterodyne spectroscopy using stabilized optical frequency combs," Phys. Rev. Lett. **100**(1), 013902 (2008) [doi:10.1103/PhysRevLett.100.013902].
[80] J.-D. Deschęnes, P. Giaccarri, and J. Genest, "Optical referencing technique with CW lasers as intermediate oscillators for continuous full delay range frequency comb interferometry," Opt. Express **18**(22), 23358–23370 (2010) [doi:10.1364/OE.18.023358].
[81] W. C. Swann et al., "Microwave generation with low residual phase noise from a femtosecond fiber laser with an intracavity electro-optic modulator," Opt Express **19**(24), 24387–24395 (2011) [doi:10.1364/OE.19.024387].
[82] H. R. Telle, B. Lipphardt, and J. Stenger, "Kerr-lens, mode-locked lasers as transfer oscillators for optical frequency measurements," Appl. Phys. B **74**(1), 1–6 (2002)

[doi:10.1007/s003400100735].
[83] J. Stenger et al., "Ultraprecise Measurement of Optical Frequency Ratios," Phys. Rev. Lett. **88**(7), 073601 (2002) [doi:10.1103/PhysRevLett.88.073601].
[84] P.-T. Ho, "Phase and amplitude fluctuations in a mode-locked laser," IEEE J. Quantum Electron. **21**(11), 1806–1813 (1985) [doi:10.1109/JQE.1985.1072594].
[85] J. P. Gordon and H. A. Haus, "Random walk of coherently amplified solitons in optical fiber transmission," Opt. Lett. **11**(10), 665 (1986) [doi:10.1364/OL.11.000665].
[86] N. R. Newbury and B. R. Washburn, "Theory of the frequency comb output from a femtosecond fiber laser," IEEE J Quantum Electron **41**(11), 1388–1402 (2005).
[87] R. Paschotta, "Noise of mode-locked lasers (Part II): timing jitter and other fluctuations," Appl. Phys. B **79**(2), 163–173 (2004) [doi:10.1007/s00340-004-1548-9].
[88] B. R. Washburn, W. C. Swann, and N. R. Newbury, "Response dynamics of the frequency comb output from a femtosecond fiber laser," Opt Express **13**(26), 10622–10633 (2005).
[89] J. A. Cox et al., "Complete characterization of quantum-limited timing jitter in passively mode-locked fiber lasers," Opt. Lett. **35**(20), 3522 (2010) [doi:10.1364/OL.35.003522].
[90] C. Kim et al., "Low timing jitter and intensity noise from a soliton Er-fiber laser mode-locked by a fiber taper carbon nanotube saturable absorber," Opt. Express **20**(28), 29524 (2012) [doi:10.1364/OE.20.029524].
[91] I. Coddington, W. C. Swann, and N. R. Newbury, "Coherent dual-comb spectroscopy at high signal-to-noise ratio," Phys Rev A **82**(4), 043817 (2010).
[92] J.-L. Peng and R.-H. Shu, "Determination of absolute mode number using two mode-locked laser combs in optical frequency metrology," Opt Express **15**(8), 4485–4492 (2007).
[93] J. Chen et al., "High repetition rate, low jitter, low intensity noise, fundamentally mode-locked 167 fs soliton Er-fiber laser," Opt Lett **32**(11), 1566–1568 (2007).
[94] Y. Le Coq et al., "Investigation of an optical frequency comb with intracavity EOM and optimization of microwave generation," April 2012, 238–241, IEEE [doi:10.1109/EFTF.2012.6502374].
[95] H. Inaba et al., "Long-term measurement of optical frequencies using a simple, robust and low-noise fiber based frequency comb," Opt. Express **14**(12), 5223–5231 (2006) [doi:10.1364/OE.14.005223].
[96] D. D. Hudson et al., "Mode-locked fiber laser frequency-controlled with an intracavity electro-optic modulator," Opt Lett **30**(21), 2948–2950 (2005).
[97] K. Iwakuni et al., "Narrow linewidth comb realized with a mode-locked fiber laser using an intra-cavity waveguide electro-optic modulator for high-speed control," Opt. Express **20**(13), 13769 (2012) [doi:10.1364/OE.20.013769].
[98] B. R. Washburn et al., "A phase locked, fiber laser-based frequency comb: limit on optical linewidth," in Conference on Lasers and Electro-Optics/International Quantum Electronics Conference and Photonic Applications Systems Technologies (2004), paper CMO3, p. CMO3, Optical Society of America (2004).
[99] H. Byun et al., "Compact, stable 1 GHz femtosecond Er-doped fiber lasers," Appl Opt **49**(29), 5577–5582 (2010) [doi:10.1364/AO.49.005577].
[100] L. C. Sinclair et al., "Fully-Stabilized All Polarization-Maintaining Fiber Erbium Frequency Comb," in Frontiers in Optics, Optical Society of America, Orlando, Florida (2013).
[101] H. Byun et al., "High-repetition-rate, 491 MHz, femtosecond fiber laser with low timing jitter," Opt. Lett. **33**(19), 2221–2223 (2008) [doi:10.1364/OL.33.002221].
[102] I. Hartl et al., "Integrated self-referenced frequency-comb laser based on a combination of fiber and waveguide technology," Opt. Express **13**(17), 6490 (2005) [doi:10.1364/OPEX.13.006490].
[103] D. Chao et al., "Self-referenced Erbium fiber laser frequency comb at a GHz repetition rate," in Optical Fiber Communication Conference and Exposition (OFC/NFOEC), 2012 and the National Fiber Optic Engineers Conference, pp. 1–3 (2012).
[104] T.-A. Liu, N. R. Newbury, and I. Coddington, "Sub-micron absolute distance measurements in sub-millisecond times with dual free-running femtosecond Er fiber-lasers," Opt. Express **19**(19), 18501–18509 (2011) [doi:10.1364/OE.19.018501].
[105] J. Lim et al., "A phase-stabilized carbon nanotube fiber laser frequency comb," Opt. Express **17**(16), 14115 (2009) [doi:10.1364/OE.17.014115].
[106] T.-H. Wu et al., "Low noise erbium fiber fs frequency comb based on a tapered-fiber carbon nanotube design," Opt. Express **19**(6), 5313 (2011) [doi:10.1364/OE.19.005313].
[107] K. Tamura, H. A. Haus, and E. P. Ippen, "Self-starting additive pulse mode-locked erbium fibre ring laser," Electron. Lett. **28**(24), 2226–2228 (1992) [doi:10.1049/el:19921430].
[108] V. J. Matsas et al., "Selfstarting passively mode-locked fibre ring soliton laser exploiting nonlinear polarisation rotation," Electron. Lett. **28**(15), 1391–1393 (1992) [doi:10.1049/el:19920885].
[109] M. Hofer et al., "Mode locking with cross-phase and self-phase modulation," Opt. Lett. **16**(7), 502 (1991) [doi:10.1364/OL.16.000502].
[110] K. Tamura et al., "Technique for obtaining high-energy ultrashort pulses from an additive-pulse mode-locked erbium-doped fiber ring laser," Opt Lett **19**(1), 46–48 (1994).
[111] H. A. Haus et al., "Stretched-pulse additive pulse mode-locking in fiber ring lasers: theory and experiment," IEEE J Quantum Electron **31**(3), 591–598 (1995) [doi:10.1109/3.364417].
[112] K. Tamura et al., "77-fs pulse generation from a stretched-pulse mode-locked all-fiber ring laser," Opt. Lett. **18**(13), 1080 (1993) [doi:10.1364/OL.18.001080].
[113] D. J. Richardson et al., "Selfstarting, passively mode-locked erbium fibre ring laser based on the amplifying Sagnac switch," Electron. Lett. **27**(6), 542–544 (1991) [doi:10.1049/el:19910341].
[114] I. I.N. Duling, "Subpicosecond all-fibre erbium laser," Electron. Lett. **27**(6), 544–545 (1991) [doi:10.1049/el:19910342].
[115] I. Duling, Irl N., "All-fiber ring soliton laser mode locked with a nonlinear mirror," Opt Lett **16**(8), 539–541 (1991).
[116] J. W. Nicholson and M. Andrejco, "A polarization maintaining, dispersion managed, femtosecond figure-eight fiber laser," Opt Express **14**(18), 8160–8167 (2006).
[117] W. D. Hänsel et al., "Laser with non-linear optical loop mirror," EP2637265 A1 (2013).
[118] W. Hänsel et al., "Ultra-low phase noise all-PM Er:fiber optical frequency comb," 2015, ATh4A.2, OSA [doi:10.1364/ASSL.2015.ATh4A.2].

[119] U. Keller, "Ultrafast solid-state laser oscillators: a success story for the last 20 years with no end in sight," Appl. Phys. B **100**(1), 15–28 (2010) [doi:10.1007/s00340-010-4045-3].
[120] U. Keller et al., "Semiconductor saturable absorber mirrors (SESAM's) for femtosecond to nanosecond pulse generation in solid-state lasers," IEEE J. Sel. Top. Quantum Electron. **2**(3), 435–453 (1996) [doi:10.1109/2944.571743].
[121] J. J. McFerran et al., "A passively mode-locked fiber laser at 1.54 μm with a fundamental repetition frequency reaching 2 GHz," Opt. Express **15**(20), 13155 (2007) [doi:10.1364/OE.15.013155].
[122] S. Wang et al., "Soliton Wake Instability in a SESAM Mode-locked Fiber Laser," in CLEO: 2014, p. SW3E.4, Optical Society of America (2014) [doi:10.1364/CLEO_SI.2014.SW3E.4].
[123] K. Wu et al., "Noise conversion from pump to the passively mode-locked fiber lasers at 15 μm," Opt. Lett. **37**(11), 1901 (2012) [doi:10.1364/OL.37.001901].
[124] N. Kuse et al., "Ultra-low noise all polarization-maintaining Er fiber-based optical frequency combs facilitated with a graphene modulator," Opt. Express **23**(19), 24342 (2015) [doi:10.1364/OE.23.024342].
[125] A. Martinez and Z. Sun, "Nanotube and graphene saturable absorbers for fibre lasers," Nat. Photonics **7**(11), 842–845 (2013) [doi:10.1038/nphoton.2013.304].
[126] S. Y. Set et al., "Ultrafast fiber pulsed lasers incorporating carbon nanotubes," IEEE J. Sel. Top. Quantum Electron. **10**(1), 137–146 (2004) [doi:10.1109/JSTQE.2003.822912].
[127] N. Nishizawa et al., "All-polarization-maintaining Er-doped ultrashort-pulse fiber laser using carbon nanotube saturable absorber," Opt Express **16**(13), 9429–9435 (2008).
[128] Z. Sun et al., "Ultrafast stretched-pulse fiber laser mode-locked by carbon nanotubes," Nano Res. **3**(6), 404–411 (2010) [doi:10.1007/s12274-010-1045-x].
[129] H. Ahmad et al., "Mode-locked L-band bismuth–erbium fiber laser using carbon nanotubes," Appl. Phys. B **115**(3), 407–412 (2013) [doi:10.1007/s00340-013-5616-x].
[130] Z. Sun et al., "Graphene Mode-Locked Ultrafast Laser," ACS Nano **4**(2), 803–810 (2010) [doi:10.1021/nn901703e].
[131] D. G. Purdie et al., "Few-cycle pulses from a graphene mode-locked all-fiber laser," Appl. Phys. Lett. **106**(25), 253101 (2015) [doi:10.1063/1.4922397].
[132] D. Popa et al., "Sub 200 fs pulse generation from a graphene mode-locked fiber laser," Appl. Phys. Lett. **97**(20), 203106 (2010) [doi:10.1063/1.3517251].
[133] S. Kim et al., "Hybrid mode-locked Er-doped fiber femtosecond oscillator with 156 mW output power," Opt. Express **20**(14), 15054–15060 (2012) [doi:10.1364/OE.20.015054].
[134] X. Li, W. Zou, and J. Chen, "419 fs hybridly mode-locked Er-doped fiber laser at 212 MHz repetition rate," Opt. Lett. **39**(6), 1553 (2014) [doi:10.1364/OL.39.001553].
[135] X. Wu et al., "Hybrid mode-locked Er-fiber oscillator with a wide repetition rate stabilization range," Appl. Opt. **54**(7), 1681 (2015) [doi:10.1364/AO.54.001681].
[136] K. Hitachi et al., "Carrier-envelope offset locking with a 2f-to-3f self-referencing interferometer using a dual-pitch PPLN ridge waveguide," Opt. Express **22**(2), 1629 (2014) [doi:10.1364/OE.22.001629].
[137] T. M. Ramond et al., "Phase-coherent link from optical to microwave frequencies by means of the broadband continuum from a 1-GHz Ti:sapphire femtosecondoscillator," Opt. Lett. **27**(20), 1842 (2002) [doi:10.1364/OL.27.001842].
[138] K. Tamura and M. Nakazawa, "Pulse compression by nonlinear pulse evolution with reduced optical wave breaking in erbium-doped fiber amplifiers," Opt. Lett. **21**(1), 68–70 (1996) [doi:10.1364/OL.21.000068].
[139] Y. Kim et al., "Er-doped fiber frequency comb with mHz relative linewidth," Opt. Express **17**(14), 11972 (2009) [doi:10.1364/OE.17.011972].
[140] L. F. Mollenauer, R. H. Stolen, and J. P. Gordon, "Experimental Observation of Picosecond Pulse Narrowing and Solitons in Optical Fibers," Phys Rev Lett **45**, 1095–1098 (1980).
[141] G. P. Agrawal, "Nonlinear Fiber Optics," in Nonlinear Science at the Dawn of the 21st Century, P. L. Christiansen, M. P. Sørensen, and A. C. Scott, Eds., pp. 195–211, Springer Berlin Heidelberg (2000).
[142] G.-R. Lin, C.-L. Pan, and Y.-T. Lin, "Self-Steepening of Prechirped Amplified and Compressed 29-fs Fiber Laser Pulse in Large-Mode-Area Erbium-Doped Fiber Amplifier," J. Light. Technol. **25**(11), 3597–3601 (2007).
[143] T. Okuno et al., "Silica-based functional fibers with enhanced nonlinearity and their applications," IEEE J. Sel. Top. Quantum Electron. **5**(5), 1385–1391 (1999) [doi:10.1109/2944.806765].
[144] M. Hirano et al., "Silica-Based Highly Nonlinear Fibers and Their Application," IEEE J Sel Top. Quantum Elecron **15**(1), 103–113 (2009) [doi:10.1109/JSTQE.2008.2010241].
[145] http://fiber-optic-catalog.ofsoptics.com/viewitems/optical--fibers/highly-nonlinear-fiber-optical-fibers1
[146] J. M. Dudley and S. Coen, "Coherence properties of supercontinuum spectra generated in photonic crystal and tapered optical fibers," Opt. Lett. **27**(13), 1180 (2002) [doi:10.1364/OL.27.001180].
[147] A. Ruehl et al., "Ultrabroadband coherent supercontinuum frequency comb," Phys Rev A **84**(1), 011806 – (2011).
[148] C. R. Menyuk et al., "Pulse dynamics in mode-locked lasers: relaxation oscillations and frequency pulling," Opt. Express **15**(11), 6677 (2007) [doi:10.1364/OE.15.006677].
[149] T. M. Fortier et al., "Generation of ultrastable microwaves via optical frequency division," Nat. Photon **5**(7), 425–429 (2011) [doi:10.1038/NPHOTON.2011.121].
[150] J. Millo et al., "Ultra-low-noise microwave extraction from fiber-based optical frequency comb," Opt Lett **34**(23), 3707–3709 (2009).
[151] F. Quinlan et al., "Ultralow phase noise microwave generation with an Er:fiber-based optical frequency divider," Opt Lett **36**(16), 3260–3262 (2011).
[152] H. Hundertmark, *Erbium fiber lasers for a frequency comb at 1560 nm*, Cuvillier Verlag (2006).
[153] W. Zhang et al., "Characterizing a fiber-based frequency comb with electro-optic modulator," IEEE Trans. Ultrason. Ferroelectr. Freq. Control **59**(3), 432–438 (2012) [doi:10.1109/TUFFC.2012.2212].
[154] H. Inaba et al., "Frequency-control characteristics of an erbium-based mode-locked fiber laser with an optically pumped ytterbium fiber," in 2015 Conference on Lasers and Electro-Optics (CLEO), pp. 1–2 (2015).
[155] M. Hoffmann, S. Schilt, and T. Südmeyer, "CEO stabilization of a femtosecond laser using a SESAM as fast opto-optical modulator," Opt. Express **21**(24), 30054 (2013) [doi:10.1364/OE.21.030054].

[156] T. C. Briles et al., "Simple piezoelectric-actuated mirror with 180 kHz servo bandwidth," Opt. Express **18**(10), 9739 (2010) [doi:10.1364/OE.18.009739].
[157] C.-C. Lee et al., "Broadband graphene electro-optic modulators with sub-wavelength thickness," Opt. Express **20**(5), 5264–5269 (2012) [doi:10.1364/OE.20.005264].
[158] S. Okubo et al., "Ultra-broadband dual-comb spectroscopy across 1.0–1.9 μm," Appl. Phys. Express **8**(8), 082402 (2015) [doi:10.7567/APEX.8.082402].
[159] S. Koke et al., "Direct frequency comb synthesis with arbitrary offset and shot-noise-limited phase noise," Nat. Photon **4**, 462 (2010).
[160] M. Zimmermann et al., "Optical clockwork with an offset-free difference-frequency comb:accuracy of sum- and difference-frequency generation," Opt. Lett. **29**(3), 310 (2004) [doi:10.1364/OL.29.000310].
[161] Y. Deng, F. Lu, and W. H. Knox, "Fiber-laser-based difference frequency generation scheme for carrier-envelope-offset phase stabilization applications," Opt. Express **13**(12), 4589 (2005) [doi:10.1364/OPEX.13.004589].
[162] T. Nakamura, I. Ito, and Y. Kobayashi, "Offset-free broadband Yb:fiber optical frequency comb for optical clocks," Opt. Express **23**(15), 19376 (2015) [doi:10.1364/OE.23.019376].
[163] F. Zhu et al., "Mid-infrared dual frequency comb spectroscopy based on fiber lasers for the detection of methane in ambient air," Laser Phys. Lett. **12**(9), 095701 (2015) [doi:10.1088/1612-2011/12/9/095701].
[164] W. Zhang et al., "Sub-100 attoseconds stability optics-to-microwave synchronization," Appl. Phys. Lett. **96**(21), 211105 (2010) [doi:10.1063/1.3431299].
[165] J. Roy et al., "Continuous real-time correction and averaging for frequency comb interferometry," Opt. Express **20**(20), 21932–21939 (2012) [doi:10.1364/OE.20.021932].
[166] T. Ideguchi et al., "Adaptive real-time dual-comb spectroscopy," Nat. Commun. **5** (2014) [doi:10.1038/ncomms4375].
[167] S. T. Dawkins, J. J. McFerran, and A. N. Luiten, "Considerations on the measurement of the stability of oscillators with frequency counters," IEEE Trans. Ultrason. Ferroelectr. Freq. Control **54**(5), 918–925 (2007) [doi:10.1109/TUFFC.2007.337].
[168] D. B. Sullivan et al., "NIST Technical Note 1337: Characterization of Clocks and Oscillators," National Institute of Standards and Technology (1990).
[169] Fred L. Walls and Andrea DeMarchi, "RF Spectrum of a Signal after Frequency Multiplication; Measurement and Comparison with Simple Calculation," IEEE Trans Instrum. Meas. **24**(3), 210–217 (1975).
[170] T. R. Schibli et al., "Attosecond active synchronization of passively mode-locked lasers by balanced cross correlation," Opt Lett **28**(11), 947–949 (2003) [doi:10.1364/OL.28.000947].